ACS NANO

www.acsnano.org

ARTICLE

Ordered Mesoporous Microcapsules from Double Emulsion Confined Block Copolymer Self-Assembly

Jörg G. Werner,* Hyomin Lee, Ulrich Wiesner, and David A. Weitz*

Cite This: *ACS Nano* 2021, 15, 3490–3499

Read Online

ACCESS | Metrics & More | Article Recommendations | Supporting Information

ABSTRACT: Polymeric microcapsules with shells containing homogeneous pores with uniform diameter on the nanometer scale are reported. The mesoporous microcapsules are obtained from confined self-assembly of amphiphilic block copolymers with a selective porogen in the shell of water-in-oil-in-water double emulsion drops. The use of double emulsion drops as a liquid template enables the formation of homogeneous capsules of 100s of microns in diameter, with aqueous cores encapsulated in a shell membrane with a tunable thickness of 100s of nanometers to 10s of microns. Microcapsules with shells that exhibit an ordered gyroidal morphology and three-dimensionally connected mesopores are obtained from the triblock terpolymer poly(isoprene)-*block*-poly(styrene)-*block*-poly(4-vinylpyridine) coassembled with pentadecylphenol as a porogen. The bicontinuous shell morphology yields nanoporous paths connecting the inside to the outside of the microcapsule after porogen removal; by contrast, one-dimensional hexagonally packed cylindrical pores, obtained from a traditional diblock copolymer system with parallel alignment to the surface, would block transport through the shell. To enable the mesoporous microcapsules to withstand harsh conditions, such as exposure to organic solvents, without rupture of the shell, we develop a cross-linking method of the nanostructured triblock terpolymer shell after its self-assembly. The microcapsules exhibit pH-responsive permeability to polymeric solutes, demonstrating their potential as a filtration medium for actively tunable macromolecular separation and purification. Furthermore, we report a tunable dual-phase separation method to fabricate microcapsules with hierarchically porous shells that exhibit ordered mesoporous membrane walls within sponge-like micron-sized macropores to further control shell permeability.

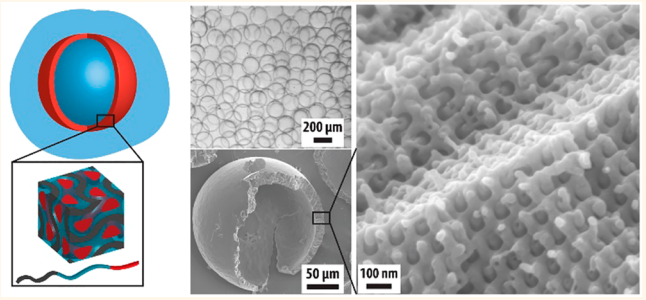

KEYWORDS: *microfluidics, gyroid, periodic nanostructure, nanoporosity, macromolecular permeability*

Microcapsules separate an interior liquid core from the external liquid environment by a thin shell membrane and represent an important architecture for advanced molecular filtration and purification methods.[1−3] Control over the transport between the two liquid spaces enables targeted molecular filtration and size-selective purification using the microcapsules and their membrane shells.[4,5] Microcapsules with homogeneous pore sizes on the scale of tens of nanometers would control the size-dependent transport of macromolecules between the liquid core and exterior as well as through a microcapsule bed or membrane based on their molar masses or hydrodynamic radii. To achieve such separation of polymers and proteins requires precise control over the selective permeability of the shell through uniform mesopores between 2 and 50 nm in diameter.[6,7] Commonly employed shell materials such as cross-linked polymers or hydrogels are able to control the transport of small molecular solutes, but their mesh size is too small for controlled mass transfer involving macromolecular species with molar masses of kilodaltons.[4] Phase separation of polymer mixtures in shells of double emulsion drops produces microcapsules with a wide range of submicron pore sizes, but microcapsules that exhibit well-controlled size-selective permeability for macromolecules with monodisperse pores on the length scale of 10s of nanometers remain elusive.[8−11] One route to achieve materials with uniform mesopores is block

Received: January 4, 2021
Accepted: February 2, 2021
Published: February 8, 2021

https://dx.doi.org/10.1021/acsnano.1c00068
ACS Nano 2021, 15, 3490–3499

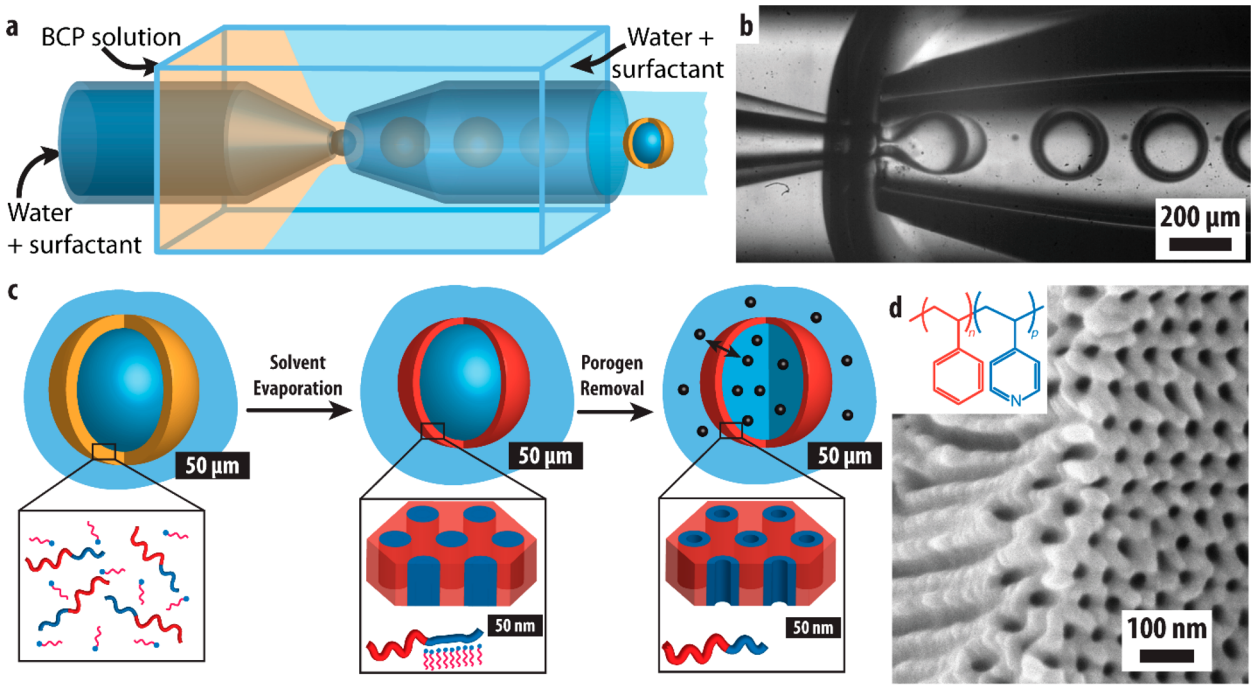

Figure 1. (a) Schematic and (b) optical microscopy image of water-in-oil-in-water double emulsion drop fabrication in a glass capillary microfluidic drop maker. Flow rates in (b) are 6, 1, and 1 mL h^{-1} for the outer aqueous, middle oil, and inner aqueous phase, respectively. (c) Schematic illustration of a double emulsion drop (left) converting to a microcapsule (middle) through solvent evaporation and simultaneous block copolymer-porogen coassembly and subsequent porogen removal (right) to fabricate ordered mesoporous microcapsules. (d) Scanning electron microscopy (SEM) image of a coassembled SV(PDP) diblock copolymer bulk film after porogen removal. Inset: chemical structure of SV.

copolymer (BCP) self-assembly that forms ordered morphologies through microphase separation of the covalently linked dissimilar polymer blocks. The self-assembly of BCPs yields well-defined nanostructures whose morphology depends on the polymer composition with length scales of 5−100 nm determined by the polymer size.[12−14] To achieve membranes from BCP self-assembly with size-selective permeability, pores have to be introduced to the initially dense BCP film that connect the two surfaces through the bulk of the material. In flat BCP membranes, common methods of introducing porosity include the selective etching of one polymer block or the inclusion of a sacrificial small molecule porogen during the self-assembly and film formation, followed by its selective dissolution, as well as combinations of BCP self-assembly with spinodal decomposition leading to hierarchical structures.[15−18] A common BCP nanostructure used for membranes contains one-dimensional porous cylinders, which require alignment perpendicular to the film to ensure connected pores throughout the membrane.[15,17] Methods to achieve alignment of BCP structures in flat membranes include the application of external electrical or magnetic fields, shear, or tuning of the preferential wetting at the substrate− and air−polymer interfaces.[17,19−23] However, these methods have only been demonstrated in flat membrane systems on solid substrates. They are not applicable to the fabrication of microcapsules from double emulsion drop templates due to the presence of only liquid−liquid interfaces and the lack of a solid substrate or air−polymer interface. Access to inorganic microcapsules with well-controlled pore size and structure directed from BCP self-assembly in the presence of two immiscible homopolymers has recently been described but is a bulk synthesis and requires substantial amounts of sacrificial organic material.[24] Research on BCP self-assembly in single emulsions, which are limited to small submicron drops, reveals the intriguing linkages and trade-offs in BCP morphology, particle shape, nanostructure orientation, and highly curved interfaces of such fully liquid systems.[25−28] However, studies on BCP self-assembly in large drops or filmlike emulsion architectures are limited and insufficient to address the challenges associated with membrane formation in mesoporous microcapsules with precise size-selective permeability for macromolecular filtration that requires control over mesopore size, orientation, and connectivity, as well as surface topology.[29,30]

Here, we report the fabrication of microcapsules with ordered nanostructured shells and connected mesopores of uniform size that exhibit size-selective permeability. We employ amphiphilic block copolymers with sacrificial porogens in the shells of water-in-oil-in-water W/O/W double emulsion drops to fabricate mesoporous microcapsules through solvent evaporation induced self-assembly. Three-dimensionally continuous mesopores that are connected throughout the shell are obtained from a triblock terpolymer system that self-assembles into a bicontinuous gyroidal morphology, while a diblock copolymer system yields hexagonally packed cylindrical mesopores aligned parallel to the membrane surface. Removal of the small molecule porogen yields uniform pore sizes in the range of 20−30 nm. To enable mesoporous microcapsules with structural integrity under harsh conditions, we develop a postassembly cross-linking strategy for the triblock terpolymer-derived gyroidal shells. We further demonstrate a method of the controlled fabrication of hierarchical macro- and mesoporous shells from dual-phase separation by tuning the salinity of the aqueous phases.

https://dx.doi.org/10.1021/acsnano.1c00068
ACS Nano 2021, 15, 3490−3499

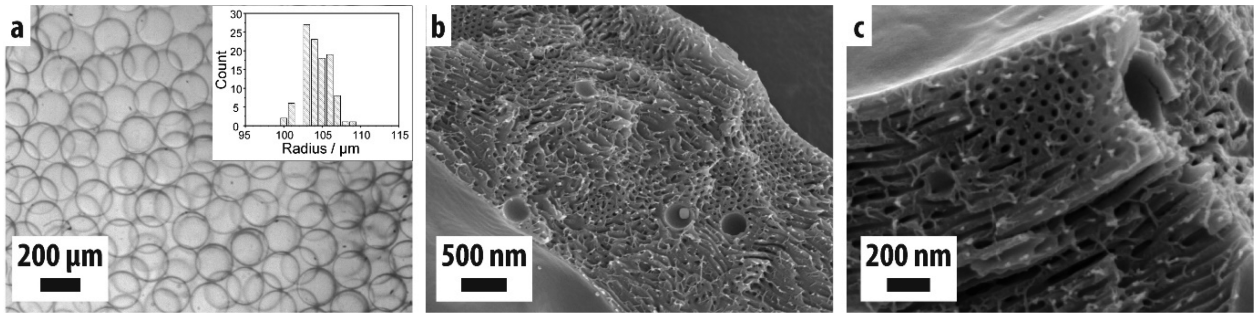

Figure 2. (a) Optical micrograph of SV(PDP) microcapsules obtained from thin-shell W/O/W double emulsion drops with 5% PVA in 1 M KCl as aqueous phase showing homogeneous capsule sizes upon solvent evaporation. Inset displays the size distribution histogram (N = 100). (b,c) Cross-sectional SEM images at different magnifications of the SV(PDP) microcapsule shells after PDP removal, exhibiting ordered mesopores with hexagonally packed cylinders aligned parallel to the shell surface.

RESULTS AND DISCUSSION

Block copolymer microcapsules are obtained from evaporating the oil of W/O/W double emulsion drops with BCP solutions as the water-immiscible oil shell. The double emulsions are fabricated in glass capillary microfluidic drop makers that enable the production of uniform double emulsions with tunable drop size, shell thickness, and phase composition.[31] The drop makers consist of two tapered cylindrical capillaries inserted into the opposite ends of a square capillary with the tapered tips facing each other and separated by 50−100 μm. Double emulsion drops are formed between the two tapered tips by flowing an inner aqueous phase through one cylindrical capillary, the BCP-containing middle oil phase through the interstitial space of the same capillary and the square capillary, and the outer aqueous phase through the interstitial space of the opposing cylindrical capillary and the square capillary, as shown in Figure 1a,b. The aqueous phases both contain poly(vinyl alcohol) as a stabilizer and viscosity enhancer. The size of the drops and the core-to-shell ratio is controlled by adjusting the flow rates of the three fluid phases. The fabrication of double emulsion drops with shells of only a few microns thickness is achieved using plug flow in the hydrophobic injection capillary, where thin oil-walled water plugs break into double emulsion drops at the tip junction.[32] Schematic representations of the microfluidic drop makers are shown in Figure 1a and Supporting Figure S1a,b. Optical microscopy images and videos of the double emulsion fabrication of various drop sizes and shell thickness are shown in Figure 1a, Supporting Figure S1c−f and Supporting Videos SV1−3.

To achieve polymer membranes with hexagonally packed cylindrical mesopores, we use the diblock copolymer poly(styrene)-*block*-poly(4-vinylpyridine) (PS-*b*-P4VP, or simply SV; M_N = 67 kg mol^{-1}, $Đ_M$ = 1.15, S: 75 wt %, V: 25 wt %) coassembled with the porogen pentadecylphenol (PDP) that selectively incorporates into the P4VP phase during self-assembly due to hydrogen bonding. The molar ratio of pyridine to phenol is kept constant at 1:1 in this study. Hexagonally packed mesoporous cylinders are obtained from the SV(PDP) diblock copolymer containing 35.2 wt % SV, 25.8 wt % PDP, and 39.0 wt % PS homopolymer (4 kg mol^{-1}), which yields a P4VP(PDP) weight fraction of 34.8 wt %. During solvent evaporation, the SV(PDP) self-assembles into hexagonally packed P4VP(PDP) cylinders embedded in a PS matrix. Subsequently, the PDP is selectively removed by dissolution in methanol to obtain porosity in the self-assembled BCP nanostructure.[17] The ordered nanostructure is preserved due to the high glass transition temperature and insolubility of the hydrophobic poly(styrene) (PS) majority block in methanol, as illustrated in Figure 1c. A scanning electron microscopy (SEM) image of the porous hexagonally packed cylinders of an SV(PDP) bulk film obtained from this composition after solvent evaporation and porogen removal with methanol is shown in Figure 1d.

To form microcapsules with shells that exhibit hexagonally packed mesopores, we use the same BCP system in the shells of double emulsion drops. Self-assembly of the BCP is induced by solvent dissipation from the oil shell while fully surrounded by the aqueous phases. We use glass capillary drop makers to fabricate thin-shell double emulsion drops whose shell phase consists of 10 wt % SV(PDP) in chloroform and with their inner and outer aqueous phases each containing 5 wt % poly(vinyl alcohol) (PVA), as a stabilizing surfactant, in 1 molar potassium chloride (KCl). The double emulsion drops are collected in an open container to allow the chloroform to dissipate, which induces self-assembly of the block copolymer and forms a solid polymeric shell. An optical microscope image of the microcapsules fabricated with a uniform size distribution and thin shells is shown in Figure 2a. The microcapsules are subsequently transferred to and washed with methanol to remove the porogen from the self-assembled nanostructured shell. Cross-sectional SEM images of the capsule shells confirm hexagonally packed nanoporous cylinders with pore diameters of approximately 30 nm, consistent with the pore size of the bulk film, as shown in Figure 2b,c and Figure 1d, respectively. The mesoporous cylinders are highly uniform throughout the entire shell, demonstrating the successful application of BCP self-assembly in double emulsion templating to fabricate ordered mesoporous shells. The morphology of the self-assembling BCP system is not altered due to the confinement to the oil shell, as shown in Figures 1d and 2c. The one-dimensional cylindrical pores are aligned parallel to the interior and exterior surfaces of the microcapsule shell, as shown in Figure 2c. For macromolecular permeability, however, connected mesopores from the capsule interior to its outer surface are desirable. In single emulsion drops, the orientation of the BCP nanostructure is due to the preferential wetting of one block to the oil−water interface and depends on the surfactant composition and interactions with the blocks: at neutral interfacial conditions, both blocks of the BCP wet the emulsion interface, which would enable shells with perpendicular cylinders to be obtained.[26] Another approach to achieve

https://dx.doi.org/10.1021/acsnano.1c00068
ACS Nano 2021, 15, 3490−3499

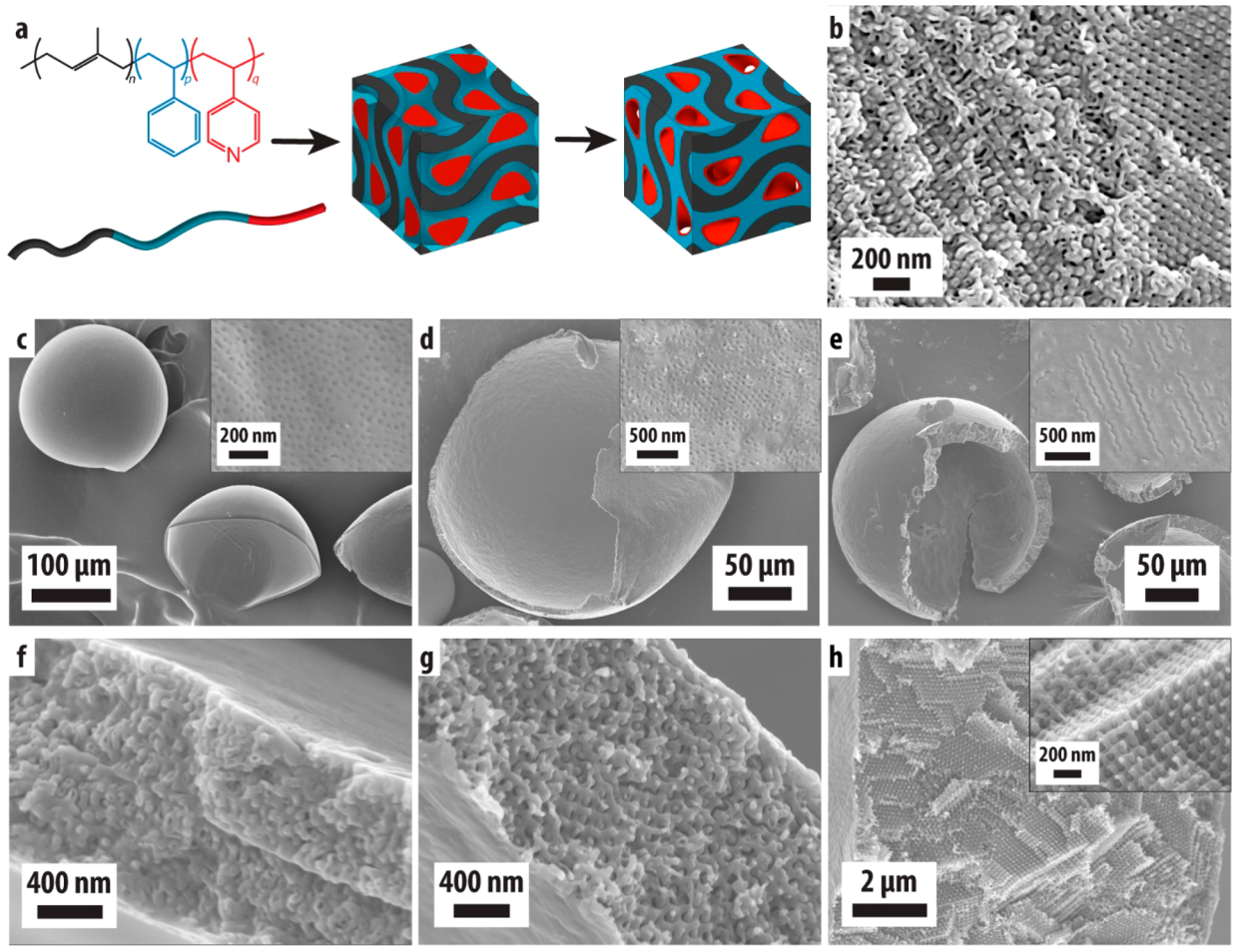

Figure 3. (a) Chemical structure of the ISV triblock terpolymer and illustrative rendering of the unit cell of a core−shell double gyroid morphology before and after removal of the minority network phases, illustrating the effect of porogen incorporation and removal from the red P4VP minority network phase (40%−35%−25% matrix-shell-networks volume fractions). (b) SEM image of a self-assembled ISV(PDP) bulk film after PDP removal showing an ordered bicontinuous mesoporous morphology. (c−h) SEM images of cross-linked ISV(PDP) microcapsules after PDP removal with (c,f) thin, (d,g) intermediate, and (e,h) thick shells. (c−e) SEM images at low magnification showing entire microcapsules after cross-sectioning. Insets show the surface of the microcapsules. (f−h) Cross-sectional SEM images of the mesoporous self-assembled shell of the triblock terpolymer microcapsules indicating the improved long-range order in thicker shells. Note that image in (f) shows the two shell sides of the thin-shell capsule collapsed onto each other due to drying.

continuous mesopores throughout the shell is the use of three-dimensionally connected porosity.

To obtain mesoporous shells whose pore structures are inherently connected throughout, we target bicontinuous nanostructures such as the gyroidal morphologies, which are accessible with BCP self-assembly. While previous studies revealed the presence of a gyroidal morphology in the SV(PDP) system, triblock terpolymers exhibit larger and experimentally more accessible phase windows for these three-dimensional morphologies as compared to diblock copolymers.[33,34] We use the triblock terpolymer poly(isoprene)-*block*-poly(styrene)-*block*-poly(4-vinylpyridine) (PI-*b*-PS-*b*-P4VP, or simply ISV; M_N = 74 kg mol^{-1}, $Đ_M$ = 1.19; I: 38 wt %, S: 44 wt %, V: 18 wt %) as the BCP to obtain a gyroidal mesoporous structure, as illustrated in Figure 3a. Bicontinuous gyroidal mesoporous networks are obtained from the ISV(PDP) triblock terpolymer system containing 54.0 wt % ISV, 27.5 wt % PDP, and 18.5 wt % PS homopolymer (4 kg mol^{-1}), which yields a P4VP(PDP) weight fraction of 37.0 wt %, as demonstrated in the SEM image of a bulk film of the triblock terpolymer system after porogen removal, shown in Figure 3b.

To fabricate microcapsules with gyroidal mesoporous shells, we use the self-assembly of the same triblock terpolymer system in double emulsion drops with varying shell thickness prepared from different microfluidic drop maker designs and flow rates, as shown in Supporting Figure S1. We fabricate microcapsules around 200 μm in diameter with shells of 700 nm, 2 μm, and 10 μm in thickness, as shown in Figure 3c−e. The shell thickness is controlled through the flow rate ratio of inner and middle phase, as well as the overall droplet size. The shell volume shrinks significantly during solvent evaporation, which manifests itself mostly in a reduction of the shell thickness. For example, the shell of the ISV thick-shelled double emulsion drops and resulting capsules shown in Figure 1b and Figure 3e,h, respectively, decreases in thickness from approximately 20 to 6−9 μm, while the diameter of the aqueous core shrinks only by about 25 μm, a 12% decrease. The cross sections of all ISV microcapsules exhibit a mesoporous three-dimensional network nanostructure throughout the microcapsule shell after porogen removal, as shown in Figure 3f−h. The thinnest shell exhibits a networked mesoporous block copolymer shell structure without long-

https://dx.doi.org/10.1021/acsnano.1c00068
ACS Nano 2021, 15, 3490−3499

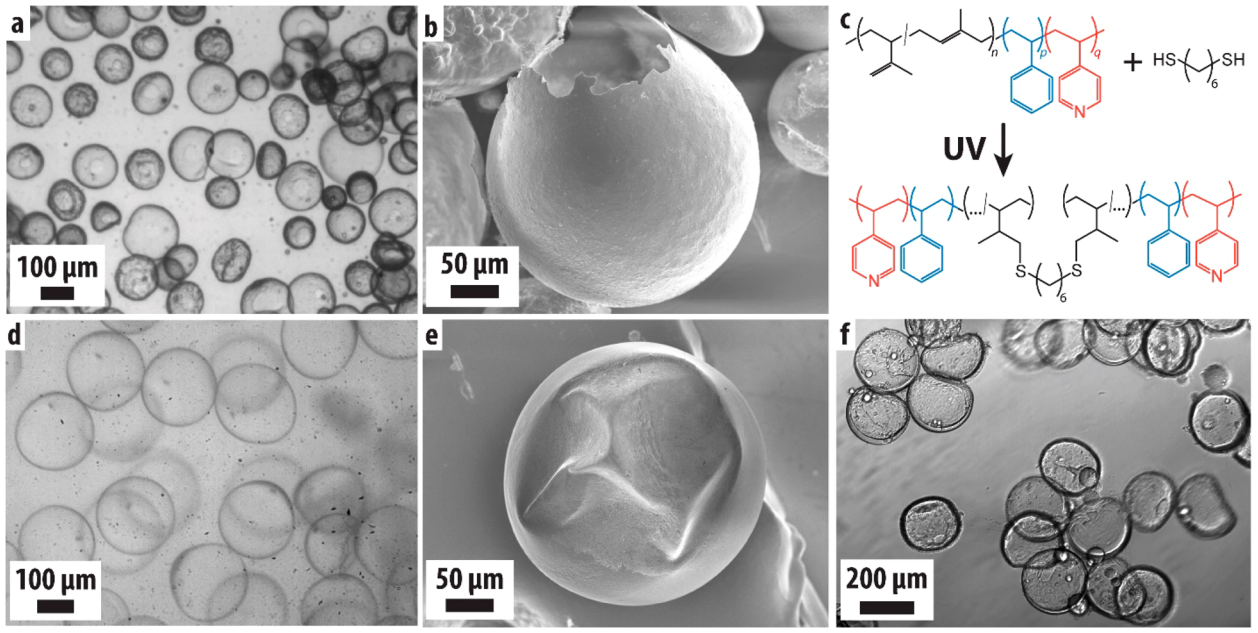

Figure 4. (a,b) Optical micrograph (a) and SEM image (b) of ISV(PDP) microcapsules after immersion in methanol for PDP removal without UV-induced thiol−ene cross-linking of the self-assembled triblock terpolymer shell. (c) Chemical cross-linking schematic of ISV triblock terpolymers using thiol−ene chemistry with difunctional cross-linkers. (d,e) Optical micrograph (d) and SEM image (e) of ISV(PDP) microcapsules after immersion in methanol for PDP removal with prior UV-induced thiol−ene cross-linking of the self-assembled triblock terpolymer shell. Capsules without cross-linking rupture upon immersion in methanol (a,b), while they stay structurally intact when cross-linked (d,e). (f) Optical micrograph of cross-linked microcapsules immersed in THF.

range order, as shown in Figure 3f. With increasing shell thickness, corresponding to longer drying time of the double emulsion drops, the long-range order of the self-assembled block copolymer nanostructure improves. At a shell thickness of 10 μm, a periodic structural order of the three-dimensional network is observed, including the presence of crystal-like facets in the cross-sectioned microcapsule shell, as shown in Figure 3h and Supporting Figure S2. As with the diblock system, the morphology of the self-assembling ISV(PDP) system is not altered due to the confinement to the oil shell, as shown in Figure 3b,h. The thin ISV shells (Figure 3f) with a thickness of only 5 times the (100) spacing of the gyroid morphology for this triblock terpolymer exhibit a disordered network morphology. However, the disorder may not be solely due to the confinement by the oil shell but also to the fast solvent removal and polymer solidification time of less than 10 min that traps the block copolymer in a disordered state.

The ordered nanostructure in the microcapsule shell consists of two interpenetrating networks with triple nodes connected by struts that contain a porous core, consistent with the double gyroid shell morphology. A simulated cross-section of the double gyroid shell morphology along the [110] direction of the gyroid unit cell and an overlay with an SEM image is shown in Supporting Figure S2, confirming the structural assignment. The cores of the networks are composed of the P4VP(PDP) phase and turn porous upon PDP porogen removal, as illustrated in Figure 3a. The shells of the networks are composed of the poly(isoprene)-*block*-poly(styrene) (PI-*b*-PS) blocks. The porous space between the networks (matrix) is due to swelling of the double gyroid structure during methanol immersion, as illustrated in Supporting Figure S2, and possibly residual solvent in the capsule shell at the time of cross-linking.[35] The surface of the thinner shells exhibit extended regions with hexagonal closed-packed pores, as well as regions where the pores are absent, as shown in the inset of Figure 3c,d and Supporting Figure S5a,b. The microcapsules with highly ordered thick shells exhibit wavelike features on the capsule surface, characteristic of the (211) gyroidal projection, combined with nonporous regions, as shown in the inset of Figure 3e and Supporting Figure S5a,b, respectively. Small-angle X-ray scattering of the microcapsules reveals a broad peak at a scattering vector q of around 0.1 nm^{-1} with a shoulder on the higher q-side and multiple broad peaks overlaid at 0.2 nm^{-1} for the thicker shells, as shown in Supporting Figure S3. The first order peak and shoulder have a q ratio of $6^{0.5}$:$8^{0.5}$, consistent with the expected first and second allowed scattering peaks corresponding to the (211) and (220) planes of the double gyroid morphology (space group $Ia\bar{3}d$, Q^{230}). The corresponding d-spacing or unit cell size of the cubic double gyroid is 155 nm, consistent with the dimensions observed in SEM.

To apply microcapsules in size-selective molecular filtration, they have to be structurally stable to prevent shell rupture under stress. The mesoporous block copolymer microcapsules do not exhibit this required mechanical integrity. For example, when exchanging the exterior aqueous phase with methanol to remove the PDP from the self-assembled shell, the large osmotic pressure that forms toward the aqueous core causes the microcapsules to burst as shown in Figure 4a,b. This behavior is due to the low degree of entanglements in our self-assembled BCPs. A strategy to enhance structural integrity of microcapsules is to use covalently cross-linked polymer shells. In order to develop a method to cross-link the BCP shell after self-assembly but before porogen removal, we utilize a difunctional thiol, hexanedithiol, that reacts with carbon−carbon double bonds of the 3,4-isoprene units in the PI block of the ISV to cross-link the self-assembled nanostructure under UV initiation, as illustrated in Figure 4c.[36] The fabrication of

https://dx.doi.org/10.1021/acsnano.1c00068
ACS Nano 2021, 15, 3490−3499

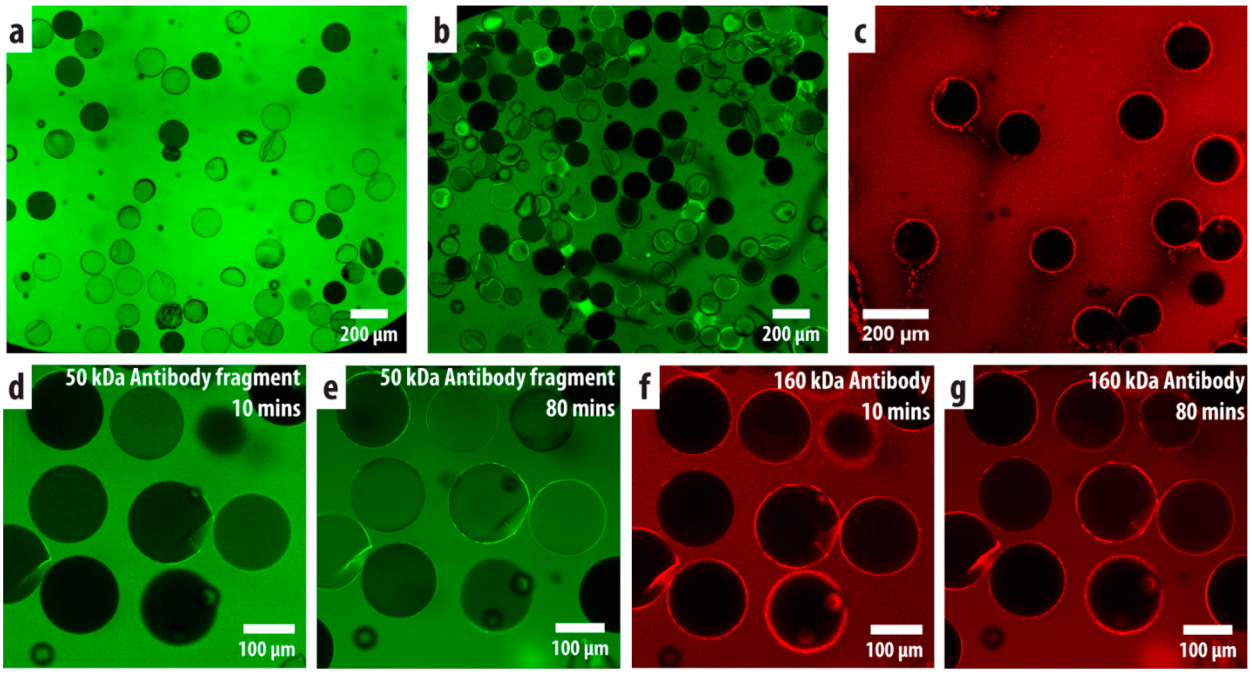

Figure 5. Permeability tests of ordered mesoporous microcapsules: (a,b) Laser-scanning fluorescence confocal (LSFC) microscopy images of thick-shell, gyroidal ISV microcapsules exposed to fluorescently labeled dextran (250 kg mol^{-1}) at (a) pH of 9 and (b) pH of 4. In alkaline condition, 68% (N = 78) of the capsules at pH 9 show permeability to the dextran, while only 47% (N = 162) were permeable in acidic environment. (c) Laser-scanning fluorescence confocal microscopy images of triblock terpolymer microcapsules challenged with fluorescently labeled poly(styrene) beads of 30 nm diameter. (d–g) LSCF microscopy images of mesoporous gyroidal ISV microcapsules exposed to fluorescently labeled (d,e) 50 kg mol^{-1} antibody Fab fragments and (f,g) 160 kg mol^{-1} whole antibodies after (d,f) 10 min exposure and (e,g) 80 min exposure.

cross-linked BCP microcapsules follows the same procedures as non-cross-linked ones with the addition of UV irradiation after solvent dissipation. Cross-linked microcapsules obtained from the ISV(PDP) triblock terpolymer system do not rupture when immersed in methanol, as shown in Figure 4d,e. The successful cross-linking of the self-assembled microcapsule shells is also evident from their insolubility in tetrahydrofuran (THF), a common solvent for all components, as shown in Figure 4f and Figure S4. The self-assembly of the block copolymer is not altered by cross-linking, and well-ordered mesoporous BCP microcapsules with structural stability for applications under harsh solution conditions are successfully fabricated.

To test the size-selective permeability of our mesoporous shells, we expose the microcapsules to fluorescently labeled dextran (250 kg mol^{-1}) with a Stokes radius of around 11.5 nm dissolved in the continuous phase and monitor the microcapsules with fluorescent scanning confocal microscopy.[37] Permeability to the macromolecular probe is indicated by increased fluorescence in the core of the capsule. Approximately two-thirds of the ISV microcapsules show uptake of the fluorescent probe to the interior of the microcapsules at pH 9, indicating porous paths connecting the inside to the outside of the microcapsule through the mesoporous shell, as evident from the confocal scanning laser microscopy image in Figure 5a. We presume that it is the inhomogeneity in surface porosity between capsules of the same architecture that causes some microcapsules to be completely blocked, preventing the permeation of the fluorescent probe through their shells. All capsule shells are impermeable, however, to 30 nm poly(styrene) particles, demonstrating no larger defects such as cracks or ruptures, as shown in Figure 5c. We further characterize the trigger-responsiveness of the shells for active manipulation of molecular permeation in and out of the microcapsule core by employing a pH-responsive BCP. As a proof-of-principle, we measure the permeability of our microcapsules to the molecular probe under acidic conditions at a pH below the pK_a of P4VP of 4.5; this causes an expansion of the P4VP polymer chains blocking the P4VP-lined mesopores and result in the impermeability of a higher fraction of microcapsules to the macromolecular probe.[6] Less than half of the ISV microcapsules are permeable to the fluorescently labeled dextran (250 kg mol^{-1}) at pH 4, as shown in Figure 5b. This is over 30% less than under alkaline conditions excluding the completely impermeable capsules. While the permeability and the pH-responsive molecular weight cut off of the shells is not uniform across the ensemble of capsules, our results demonstrate that the macromolecular selectivity is altered in some ISV microcapsules using pH as a controlled stimulus. In contrast to the uniform porosity and ordered nanostructure throughout the shell, the topography and porosity of the shell surface are heterogeneous around the outside of a single capsule, as well as between capsules of the same kind, as shown in the surface SEM images in Supporting Figure S5. We speculate that the nonuniform permeability and pH-response between mesoporous BCP microcapsules of the same architecture is likely further improved by controlling the parameters influencing the homogeneity of the surface porosity.

The permeation and rejection of biologically relevant molecules such as proteins is of particular interest for ultrafiltration applications. To test biomolecular differentiation in the permeability of the gyroidal mesoporous ISV microcapsules, the capsules are exposed to fluorescently labeled

https://dx.doi.org/10.1021/acsnano.1c00068
ACS Nano 2021, 15, 3490–3499

whole IgG antibodies (160 kg mol^{-1}) as well as Fab antibody fragments (50 kg mol^{-1}) and monitored with fluorescent scanning confocal microscopy over time. While the smaller antibody fragment is detected inside the capsules within 10 min, and permeated most capsules after 80 min, as shown in Figure 5d,e, fluorescence from the larger whole antibody is not observed inside the same capsules over the same time frame. Such a size-dependent permeability and capture time is expected for membranes with mesopores that are in the same size range as the biomacromolecules. Again, the heterogeneity in permeability across the ensemble of microcapsules is evident from the nonuniform increase in fluorescence of the small antibody fragment in the cores of the microcapsules over time, as can be seen in Figure 5d,e.

Shell membranes with high permeability and fast diffusion of the filtrate are highly desirable for efficient separation. Hierarchically porous structures that include macropores enable fast flux and diffusion in nanoporous membranes.[38] We achieve hierarchically structured shells with nanometer- and micrometer-sized pores from a dual phase separation process: microphase separation of BCPs combined with self-emulsification of small water droplets into the oil shell that is controlled through the salt concentration in the aqueous phases. Microcapsules with shells comprising a connected sponge-like morphology with micron-sized pores in addition to ordered mesoporous structures from SV BCP self-assembly are fabricated from W/O/W double emulsion drops with inner and outer aqueous phases containing 5 wt % PVA without the addition of salt. While the drops are optically transparent immediately after fabrication, the capsules exhibit strong scattering of light and appear dark in transmission, as shown in Figure 6a. The strong scattering demonstrates the formation of structural features on length scales comparable to the wavelength of visible light. Cross-sectional SEM reveals that the SV BCP self-assembles into nanoporous cylinders in the shell between large micron-sized voids, as shown in Figure 6b,c. The voids originate from the self-emulsified water drops inside the oil shell that form during the solvent evaporation and block copolymer self-assembly, as previously observed in toluene-in-water single emulsion drops containing SV.[28] At low salinity, water diffuses into the oil shells on the molecular level and in inverse block copolymer micelles, and as the organic solvent chloroform dissipates, the water concentration increases beyond its solubility limit, inducing phase separation and growth of water drops inside the oil shell, as illustrated in Figure 6d.[39,40] At high salinity, this process of self-emulsification is suppressed. The tunable self-emulsification of water into the oil shells in combination with BCP self-assembly enables the controlled formation of hierarchically macro- and mesoporous microcapsules that might combine fast diffusion kinetics with nanometer size-resolution for targeted macromolecular separation.

CONCLUSION

We report the successful use of block copolymer self-assembly with a small molecule porogen confined in the oil shell of double emulsion drops to fabricate microcapsules with ordered nanoporous shells. Highly uniform mesopores that connect the exterior to the capsule core are obtained from a triblock terpolymer that self-assembles into the bicontinuous double gyroid morphology, yielding size-selective permeability on the length scale of 10s of nanometers with pH-responsiveness. We find that the confinement of the block copolymer inside the oil

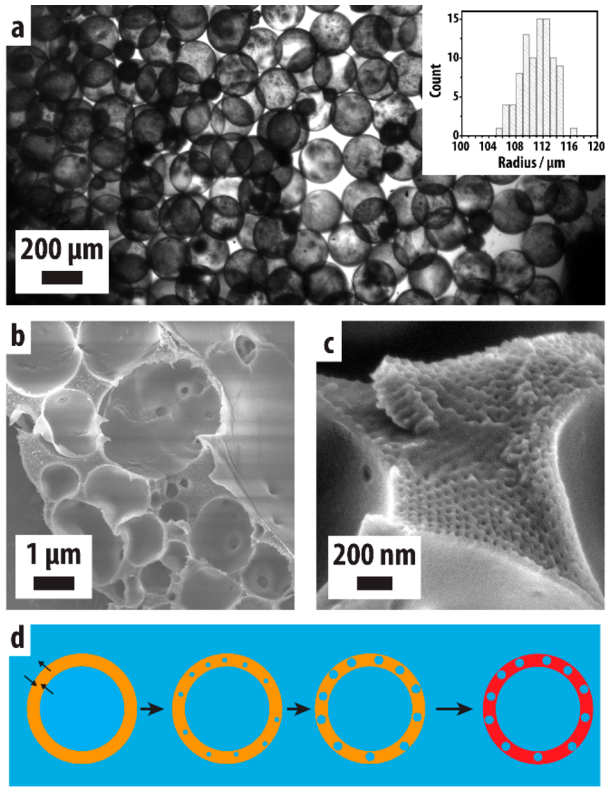

Figure 6. (a) Optical micrograph of dual-phase separated SV(PDP) microcapsules obtained from double emulsion drops with 5 wt % PVA as the aqueous phases showing the optical scattering of the capsules upon solvent evaporation. Inset shows the size distribution histogram of the capsules (N = 90). (b,c) Cross-sectional SEM images at different magnifications of the shell of the SV(PDP) microcapsules after PDP removal showing micron-sized pores in the shell (b) with mesopores in the walls between them (c) exhibiting a hexagonally packed cylindrical morphology. (d) Schematic illustration of self-emulsification of water drops inside the oil shell during solvent evaporation that leads to the micron-sized voids and optical scattering in the block copolymer microcapsules.

shell of the double emulsion droplets does not impact their self-assembled lattice formation. We further demonstrate a tunable dual-phase separation method for hierarchical shell architectures by tuning the aqueous surrounding environment during self-assembly of the amphiphilic block copolymers in the oil shell: macro- and mesoporous shells are obtained through self-emulsification and phase separation of micron-sized water drops inside the oil shell at low salinity. Cross-linking of the self-assembled nanostructured shell endows the microcapsules with structural integrity that enables both handling under various chemical conditions and stimuli responsive behavior. The gyroidal mesoporous microcapsules fabricated with pH-dependent permeability have potential applications in macromolecular separation and purification: microcapsules with well-defined mesopores can significantly increase the efficiency of size exclusion chromatography, where small macromolecules are separated from larger ones due to their increased residence time in smaller pores when flowing through a bed of porous particles. The difference in explorable volume, and hence elution volume, is orders of magnitude larger if microcapsules with mesoporous shell membranes are used instead of solid-cored porous particles. This difference in

https://dx.doi.org/10.1021/acsnano.1c00068
ACS Nano 2021, 15, 3490−3499

elution volume would increase chromatography resolution and decrease necessary column length. Furthermore, the method of obtaining high-aspect ratio films with thicknesses of 100s of nanometers to microns without a solid substrate represents a nontraditional approach to study amphiphilic block copolymer self-assembly. The soft and dynamically tunable nature of the liquid substrate of the double emulsion drop will enable the study of interfacial curvature and chemical gradients across a liquid film on the nanostructure formation; diffusion of molecules between the aqueous core and exterior may influence the alignment of the BCP morphology. Scattering experiments during solvent evaporation and BCP film formation in the liquid emulsion drop confinement likely can be used to probe the self-assembly process without the interference of solid substrates. Thus, these microcapsules with controlled porosity should prove useful both for fundamental studies of BCP self-assembly as well as macromolecular separation applications.

METHODS

Materials. Poly(vinyl alcohol) (M_w 13000−23000, 87−89% hydrolyzed, PVA), poly(styrene) (PS, analytical standard, for GPC, 4,000 g mol^{-1}), 2-hydroxy-2-methylpropiophenone (Darocure 1173), 1,6-hexanedithiol (≥97%), chloroform (anhydrous, contains amylenes as stabilizer, ≥99%), tetrahydrofuran (THF, anhydrous, ≥99.9%, inhibitor-free), potassium chloride (for molecular biology, ≥99.0%), and octadecyltrimethoxysilane (technical grade, 90%, ODTS) were purchased from Sigma-Aldrich and used as received. 3-Pentedecylphenol (technical grade, 90%) was purchased from Sigma-Aldrich and recrystallized from diethyl ether before use. The fluorescent probe fluorescein isothiocyanate-dextran (FITC-dextran) with a molecular weight of 250000 g mol^{-1} was purchased from Sigma-Aldrich and used as received at 1 mg mL^{-1} in DI-water. The hydrophilic silane 2-(methoxy(polyethyleneoxy)propyl)trimethoxysilane was purchased from Gelest and used as received. Permeation measurements at pH 4 and pH 9 were done with BDH pH Reference Standard Buffers. The diblock copolymer poly(styrene)-*block*-poly(4-vinylpyridine) (SV, PS-P4VP, M_N = 67 kg mol^{-1}, $Đ_M$ = 1.15, 25 wt % P4VP) was purchased from Polymer Source (P9823-S4VP) and used as received.

Synthesis of ISV Triblock Terpolymer. The poly(isoprene)-*block*-poly(styrene)-*block*-poly(4-vinylpyridine) triblock terpolymer (ISV) used here was synthesized using sequential anionic polymerization as described in detail previously.[6] The molecular weight of the ISV used was M_N = 74 kg mol^{-1} ($Đ_M$ = 1.19) with weight fractions of f_w = 38%, 44.5%, and 17.6% for I, S, and V, respectively.

Fabrication of Double Emulsion Drops and Microcapsules. Double emulsion drops were fabricated using glass capillary microfluidic drop makers, as illustrated in Figure S1a,b. The devices consist of two tapered cylindrical capillaries aligned inside a square capillary with an inner dimension slightly larger than that of the outer diameter of the cylindrical capillaries (1 mm). One cylindrical capillary with a smaller tapered tip, termed the injection capillary, is rendered hydrophobic by treating it with ODTS for 1 h. To prevent the wetting of the double emulsion drops on the second cylindrical capillary, termed the outlet capillary, it is rendered hydrophilic by treating it with 2-(methoxy(polyethyleneoxy)propyl)trimethoxysilane for 1 h. For thin-shell capsules, an additional flame-pulled cylindrical capillary is inserted into the hydrophobic injection capillary from its nontapered end. The open ends of all but the outlet capillary are capped with 20 G blunt needles as tube connections that are sealed to a glass slide with 5 min epoxy (Devcon).

To form thick-shell double emulsion drops, the inner aqueous phase is injected through the hydrophobically treated injection capillary, while the middle shell phase is injected from the same direction through the interstitial space between the square capillary and the injection capillary. The outer aqueous phase is injected from the opposite direction, also through the interstitial space between the square capillary and outlet capillary, as illustrated in Figure S1a. Thin-shell double emulsion drops are obtained by injecting the inner aqueous phase through the flame-pulled innermost capillary (composition described in text), the block copolymer middle phase through the cylindrical injection capillary, and the aqueous outer phase through the interstitial space between the square and the outlet capillary, as illustrated in Figure S1b. Drop formation in the glass capillary device is monitored with a fast camera (Phantom V9.0) on a Leica inverted optical microscope. Double emulsion drops are formed between the tapered cylindrical capillary tips in the dripping regime at various flow rates described in the text. Following drop breakup, the double emulsion drops flow through the cylindrical outlet capillary and are collected in glass dish filled with outer aqueous phase of 2 mm in height (e.g., 5 wt % PVA in water, or 5 wt % PVA in aqueous 1 M KCl). The composition of the oil phase is 10 wt % SV(PDP) + PS (4 kg mol^{-1}) in chloroform for hexagonally packed cylinders, and 10 wt % ISV(PDP) + PS (4 kg mol^{-1}) in 7:3 by volume chloroform:tetrahydrofuran for double gyroidal shells with the addition of 1.4 vol % hexanedithiol and 2-hydroxy-2-methylpropiophenone each for cross-linked gyroidal ISV triblock terpolymer microcapsules. Lower polymer concentrations in the shell phase are empirically found to yield significant shell rupture during solvent evaporation.

The double emulsion drops are dried by evaporation of the shell solvent (approximately 10 min for thin, 30 min for medium, and 3 h for thick shells) in open atmosphere. For cross-linking of the block copolymer shells containing hexanedithiol, the capsules are exposed to UV light for 1 min (Omnicure S1500, >350 nm, 4 cm distance, approximately 400 mW cm^{-2}). Thick-shelled double emulsion drops rupture if left for evaporation over a longer time period, and UV cross-linking is done before rupturing takes place, likely causing residual solvent to be present during the cross-linking process. Subsequently, the capsules are washed and immersed in excess methanol for 24 h for porogen (PDP) removal. After methanol extraction, the capsules are washed three times with and subsequently kept in DI-water for characterization.

Characterization of Microcapsules. Microcapsules for scanning electron microscopy (SEM) analysis are prepared by drying aliquots of microcapsules from DI-water in air on double-sided adhesive conductive carbon tape. Some dried microcapsules for SEM are cross-sectioned with a razor blade after drying. Prior to imaging, the SEM samples are sputter-coated with a thin layer (5 nm) of platinum/palladium (Pt:Pd 80:20) using a sputter coater (EMS 300T D dual head sputter coater). The microcapsules are imaged using a field emission scanning electron microscope (FESEM, Zeiss UltraPlus) equipped with an in-lens detector at an accelerating voltage of 3 kV. Small angle X-ray (SAXS) measurements of the capsules dispersed in water were performed at the line G1 of the Cornell High Energy Synchrotron Source (CHESS). The sample to detector distance was 2.5 m and the X-ray wavelength λ was 1.2545 Å with a beam size of approximately 250 × 250 μm^2. The scattering vector q is defined as $q = (4\pi/\lambda) \sin \theta$ where θ is half of the scattering angle. A Pilatus 300k detector was used to record the 2D small-angle X-ray scattering (SAXS) patterns.

Permeability Measurements. Microcapsule permeability under various pH conditions is characterized using molecular permeation into the capsule interior of FITC-dextran (250000 g mol^{-1}) at a concentration of 1 mg mL^{-1}. To a well in a 96-well plate containing the microcapsules in the respective buffer solution of desired pH (100 μL), the dye−dextran solution is added (20 μL) and incubated for at least 18 h. The permeability of the capsules is then characterized using a laser confocal fluorescent microscope (Leica Microsystems SP-5) with an excitation wavelength of 488 nm and detector wavelength range of 490−540 nm. The microcapsules are similarly characterized toward their time-resolved permeability of antibodies (Alexa Fluor 594 AffiniPure Goat Anti-Rat IgG, 160 kg mol^{-1}, Jackson ImmunoResearch 112−585−072) at a concentration of 0.01 mg mL^{-1} and Fab fragment antibodies (Alexa Fluor 488 AffiniPure Fab Fragment Goat Anti-Mouse IgG (H+L), 50 kg mol^{-1}, Jackson ImmunoResearch 115−547−003) at a concentration of 0.03 mg mL^{-1} in phosphate-buffered saline (PBS, pH = 7.4). After adding the

https://dx.doi.org/10.1021/acsnano.1c00068
ACS Nano 2021, 15, 3490−3499

fluorescently labeled antibody fragments and whole antibodies to the well plate containing the capsules, the capsules are monitored using a laser confocal fluorescent microscope (Leica Microsystems SP-5) with excitation wavelengths of 488 and 633 nm and detector wavelength ranges of 490−530 and 635−700 nm, respectively.

ASSOCIATED CONTENT

Supporting Information

The Supporting Information is available free of charge at https://pubs.acs.org/doi/10.1021/acsnano.1c00068.

SEM images of gyroidal microcapsule shells and surfaces, and small-angle X-ray scattering patterns of gyroidal microcapsules, contained in Supporting Figures S1−S5 (PDF)

High speed optical microscopy video of thick-shell double emulsion fabrication (AVI)

High speed optical microscopy video of medium-shell double emulsion fabrication (AVI)

High speed optical microscopy video of thin-shell double emulsion fabrication (AVI)

AUTHOR INFORMATION

Corresponding Authors

Jörg G. Werner − *John A. Paulson School of Engineering and Applied Sciences, Harvard University, Cambridge, Massachusetts 02138, United States; Department of Mechanical Engineering and Division of Materials Science and Engineering, Boston University, Boston, Massachusetts 02215, United States;* orcid.org/0000-0001-7845-086X; Email: jgwerner@bu.edu

David A. Weitz − *John A. Paulson School of Engineering and Applied Sciences, Harvard University, Cambridge, Massachusetts 02138, United States; Department of Physics, Harvard University, Cambridge, Massachusetts 02138, United States;* orcid.org/0000-0001-6678-5208; Email: weitz@seas.harvard.edu

Authors

Hyomin Lee − *John A. Paulson School of Engineering and Applied Sciences, Harvard University, Cambridge, Massachusetts 02138, United States; Department of Chemical Engineering, Pohang University of Science and Technology, Pohang, Gyeongbuk 37673, Republic of Korea;* orcid.org/0000-0002-0968-431X

Ulrich Wiesner − *Department of Materials Science and Engineering, Cornell University, Ithaca, New York 14850, United States;* orcid.org/0000-0001-6934-3755

Complete contact information is available at: https://pubs.acs.org/10.1021/acsnano.1c00068

Notes

The authors declare no competing financial interest.

ACKNOWLEDGMENTS

This work was supported by the National Science Foundation (Grant No. DMR-1708729). This work was performed in part at the Harvard MRSEC (Grant No. DMR-1420570) and the Center for Nanoscale Systems (CNS), a member of the National Nanotechnology Coordinated Infrastructure Network (NNCI), which is supported by the National Science Foundation under NSF Award No. 1541959. CNS is part of Harvard University. H.L. acknowledges support from the National Research Foundation of Korea (NRF) grant funded by the Korean government (MSIT) (No. 2020R1C1C1004642). U. Wiesner acknowledges the support of the NSF (Grant No. DMR-1707836). This work is partially based upon research conducted at the Cornell High Energy Synchrotron Source (CHESS), which is supported by the National Science Foundation and the National Institutes of Health/National Institute of General Medical Sciences under NSF award DMR-1829070, using the Macromolecular Diffraction at CHESS (MacCHESS) facility, which is supported by award GM-124166 from the National Institutes of Health, through its National Institute of General Medical Sciences.

REFERENCES

(1) Lee, T. Y.; Choi, T. M.; Shim, T. S.; Frijns, R. A.; Kim, S. H. Microfluidic Production of Multiple Emulsions and Functional Microcapsules. *Lab Chip* **2016**, *16* (18), 3415−3440.

(2) Tokarev, I.; Minko, S. Stimuli-Responsive Porous Hydrogels at Interfaces for Molecular Filtration, Separation, Controlled Release, and Gating in Capsules and Membranes. *Adv. Mater.* **2010**, *22* (31), 3446−3462.

(3) Liu, J.; Chen, H.; Shi, X.; Nawar, S.; Werner, J. G.; Huang, G.; Ye, M.; Weitz, D. A.; Solovev, A. A.; Mei, Y. Hydrogel Microcapsules with Photocatalytic Nanoparticles for Removal of Organic Pollutants. *Environ. Sci.: Nano* **2020**, *7* (2), 656−664.

(4) Werner, J. G.; Deveney, B. T.; Nawar, S.; Weitz, D. A. Dynamic Microcapsules with Rapid and Reversible Permeability Switching. *Adv. Funct. Mater.* **2018**, *28* (39), 1803385.

(5) Werner, J. G.; Nawar, S.; Solovev, A. A.; Weitz, D. A. Hydrogel Microcapsules with Dynamic Ph-Responsive Properties from Methacrylic Anhydride. *Macromolecules* **2018**, *51* (15), 5798−5805.

(6) Phillip, W. A.; Dorin, R. M.; Werner, J. G.; Hoek, E. M. V.; Wiesner, U.; Elimelech, M. Tuning Structure and Properties of Graded Triblock Terpolymer-Based Mesoporous and Hybrid Films. *Nano Lett.* **2011**, *11* (7), 2892−2900.

(7) Dorin, R. M.; Phillip, W. A.; Sai, H.; Werner, J. G.; Elimelech, M.; Wiesner, U. Designing Block Copolymer Architectures for Targeted Membrane Performance. *Polymer* **2014**, *55* (1), 347−353.

(8) Kim, B.; Lee, T. Y.; Abbaspourrad, A.; Kim, S.-H. Perforated Microcapsules with Selective Permeability Created by Confined Phase Separation of Polymer Blends. *Chem. Mater.* **2014**, *26* (24), 7166−7171.

(9) Kim, B.; Jeon, T. Y.; Oh, Y. K.; Kim, S. H. Microfluidic Production of Semipermeable Microcapsules by Polymerization-Induced Phase Separation. *Langmuir* **2015**, *31* (22), 6027−6034.

(10) Wang, B.; Prinsen, P.; Wang, H.; Bai, Z.; Wang, H.; Luque, R.; Xuan, J. Macroporous Materials: Microfluidic Fabrication, Functionalization and Applications. *Chem. Soc. Rev.* **2017**, *46* (3), 855−914.

(11) Loiseau, E.; Niedermair, F.; Albrecht, G.; Frey, M.; Hauser, A.; Ruhs, P. A.; Studart, A. R. Strong Microcapsules with Permeable Porous Shells Made through Phase Separation in Double Emulsions. *Langmuir* **2017**, *33* (9), 2402−2410.

(12) Leibler, L. Theory of Microphase Separation in Block Copolymers. *Macromolecules* **1980**, *13* (6), 1602−1617.

(13) Matsen, M. W. Self-Assembly of Block Copolymers in Thin Films. *Curr. Opin. Colloid Interface Sci.* **1998**, *3* (1), 40−47.

(14) Mai, Y.; Eisenberg, A. Self-Assembly of Block Copolymers. *Chem. Soc. Rev.* **2012**, *41* (18), 5969−5985.

(15) Phillip, W. A.; O'Neill, B.; Rodwogin, M.; Hillmyer, M. A.; Cussler, E. L. Self-Assembled Block Copolymer Thin Films as Water Filtration Membranes. *ACS Appl. Mater. Interfaces* **2010**, *2* (3), 847−853.

(16) Ikkala, O.; ten Brinke, G. Functional Materials Based on Self-Assembly of Polymeric Supramolecules. *Science* **2002**, *295* (5564), 2407−2409.

(17) Mäki-Ontto, R.; de Moel, K.; de Odorico, W.; Ruokolainen, J.; Stamm, M.; ten Brinke, G.; Ikkala, O. Hairy Tubes": Mesoporous

Materials Containing Hollow Self-Organized Cylinders with Polymer Brushes at the Walls. *Adv. Mater.* **2001**, *13* (2), 117−121.
(18) Sai, H.; Tan, K. W.; Hur, K.; Asenath-Smith, E.; Hovden, R.; Jiang, Y.; Riccio, M.; Muller, D. A.; Elser, V.; Estroff, L. A.; Gruner, S. M.; Wiesner, U. Hierarchical Porous Polymer Scaffolds from Block Copolymers. *Science* **2013**, *341* (6145), 530−534.
(19) Rokhlenko, Y.; Moschovas, D.; Miskaki, C.; Chan, E. P.; Avgeropoulos, A.; Osuji, C. O. Creating Aligned Nanopores by Magnetic Field Processing of Block Copolymer/Homopolymer Blends. *ACS Macro Lett.* **2019**, *8* (3), 261−266.
(20) van Zoelen, W.; Asumaa, T.; Ruokolainen, J.; Ikkala, O.; ten Brinke, G. Phase Behavior of Solvent Vapor Annealed Thin Films of PS-b-P4VP(PDP) Supramolecules. *Macromolecules* **2008**, *41* (9), 3199−3208.
(21) Park, S.; Kim, Y.; Lee, W.; Hur, S.-M.; Ryu, D. Y. Gyroid Structures in Solvent Annealed PS-b-PMMA Films: Controlled Orientation by Substrate Interactions. *Macromolecules* **2017**, *50* (13), 5033−5041.
(22) Morkved, T. L.; Lu, M.; Urbas, A. M.; Ehrichs, E. E.; Jaeger, H. M.; Mansky, P.; Russell, T. P. Local Control of Microdomain Orientation in Diblock Copolymer Thin Films with Electric Fields. *Science* **1996**, *273* (5277), 931−933.
(23) Darling, S. B. Directing the Self-Assembly of Block Copolymers. *Prog. Polym. Sci.* **2007**, *32* (10), 1152−1204.
(24) Hwang, J.; Kim, S.; Wiesner, U.; Lee, J. Generalized Access to Mesoporous Inorganic Particles and Hollow Spheres from Multicomponent Polymer Blends. *Adv. Mater.* **2018**, *30* (27), No. e1801127.
(25) Yan, N.; Zhu, Y.; Jiang, W. Recent Progress in the Self-Assembly of Block Copolymers Confined in Emulsion Droplets. *Chem. Commun.* **2018**, *54* (94), 13183−13195.
(26) Jang, S. G.; Audus, D. J.; Klinger, D.; Krogstad, D. V.; Kim, B. J.; Cameron, A.; Kim, S. W.; Delaney, K. T.; Hur, S. M.; Killops, K. L.; Fredrickson, G. H.; Kramer, E. J.; Hawker, C. J. Striped, Ellipsoidal Particles by Controlled Assembly of Diblock Copolymers. *J. Am. Chem. Soc.* **2013**, *135* (17), 6649−6657.
(27) Ku, K. H.; Shin, J. M.; Yun, H.; Yi, G. R.; Jang, S. G.; Kim, B. J. Multidimensional Design of Anisotropic Polymer Particles from Solvent-Evaporative Emulsion. *Adv. Funct. Mater.* **2018**, *28* (42), 1802961.
(28) Ku, K. H.; Shin, J. M.; Klinger, D.; Jang, S. G.; Hayward, R. C.; Hawker, C. J.; Kim, B. J. Particles with Tunable Porosity and Morphology by Controlling Interfacial Instability in Block Copolymer Emulsions. *ACS Nano* **2016**, *10* (5), 5243−5251.
(29) Shim, J. W.; Kim, S.-H.; Jeon, S.-J.; Yang, S.-M.; Yi, G.-R. Microcapsules with Tailored Nanostructures by Microphase Separation of Block Copolymers. *Chem. Mater.* **2010**, *22* (19), 5593−5600.
(30) Xu, J.; Li, J.; Yang, Y.; Wang, K.; Xu, N.; Li, J.; Liang, R.; Shen, L.; Xie, X.; Tao, J.; Zhu, J. Block Copolymer Capsules with Structure-Dependent Release Behavior. *Angew. Chem., Int. Ed.* **2016**, *55* (47), 14633−14637.
(31) Utada, A. S.; Lorenceau, E.; Link, D. R.; Kaplan, P. D.; Stone, H. A.; Weitz, D. A. Monodisperse Double Emulsions Generated from a Microcapillary Device. *Science* **2005**, *308* (5721), 537−541.
(32) Arriaga, L. R.; Amstad, E.; Weitz, D. A. Scalable Single-Step Microfluidic Production of Single-Core Double Emulsions with Ultra-Thin Shells. *Lab Chip* **2015**, *15* (16), 3335−3340.
(33) Tyler, C. A.; Qin, J.; Bates, F. S.; Morse, D. C. SCFT Study of Nonfrustrated ABC Triblock Copolymer Melts. *Macromolecules* **2007**, *40* (13), 4654−4668.
(34) Vukovic, I.; Voortman, T. P.; Merino, D. H.; Portale, G.; Hiekkataipale, P.; Ruokolainen, J.; ten Brinke, G.; Loos, K. Double Gyroid Network Morphology in Supramolecular Diblock Copolymer Complexes. *Macromolecules* **2012**, *45* (8), 3503−3512.
(35) Yin, J.; Yao, X.; Liou, J. Y.; Sun, W.; Sun, Y. S.; Wang, Y. Membranes with Highly Ordered Straight Nanopores by Selective Swelling of Fast Perpendicularly Aligned Block Copolymers. *ACS Nano* **2013**, *7* (11), 9961−9974.
(36) Ten Brummelhuis, N.; Diehl, C.; Schlaad, H. Thiol−Ene Modification of 1, 2-Polybutadiene Using UV Light or Sunlight. *Macromolecules* **2008**, *41* (24), 9946−9947.
(37) Armstrong, J. K.; Wenby, R. B.; Meiselman, H. J.; Fisher, T. C. The Hydrodynamic Radii of Macromolecules and Their Effect on Red Blood Cell Aggregation. *Biophys. J.* **2004**, *87* (6), 4259−4270.
(38) Peinemann, K. V.; Abetz, V.; Simon, P. F. Asymmetric Superstructure Formed in a Block Copolymer *via* Phase Separation. *Nat. Mater.* **2007**, *6* (12), 992−996.
(39) Zhu, J.; Hayward, R. C. Interfacial Tension of Evaporating Emulsion Droplets Containing Amphiphilic Block Copolymers: Effects of Solvent and Polymer Composition. *J. Colloid Interface Sci.* **2012**, *365* (1), 275−279.
(40) Etienne, G.; Vian, A.; Biočanin, M.; Deplancke, B.; Amstad, E. Cross-Talk between Emulsion Drops: How Are Hydrophilic Reagents Transported across Oil Phases? *Lab Chip* **2018**, *18* (24), 3903−3912.

https://dx.doi.org/10.1021/acsnano.1c00068
ACS Nano 2021, 15, 3490−3499